MODELING THE CHARACTERISTICS OF ELECTRON BEAMS AND SECONDARY PHOTONS WHEN PASSING THROUGH AN AIR LAYER

E.V. Oleinikov[1], E.Yu. Remeta[1], O.I. Gomonai[1], Yu.Yu. Bilak[2]
[1]Institute of electron physics NAS of Ukraine, Uzhhorod, Ukraine;
[2]Uzhhorod National University, Uzhhorod, Ukraine

Reliable information on the characteristics (spectral, integral, spatial distributions) of electron beams and secondary photons hitting the plane of sample potential placement during their irradiation at accelerators is necessary for the optimization procedure and prediction of experimental results. The results of simulations of the influence of air layers (1…5000 mm) between the electron output node of the M-30 microtron and the potential plane (1000×1000 mm) on the characteristics of the primary electron beam with an energy of 17.5 MeV and the generated secondary bremsstrahlung photons are presented. When modeling with the GEANT4 tool, the technical characteristics of the M-30 microtron were taken into account.

PACS: 29.17.+w, 29.27._a

INTRODUCTION

Beams of electron accelerators of various types are used to solve a wide range of applied problems related to multiple aspects of human life [1]. For their successful use, reliable and accurate information is required about their initial characteristics (energy, spectral, integral, spatial distributions [2]), possible changes in these characteristics in the process of transporting particles to the irradiation objects and interacting with the irradiated samples themselves [3-6]. It should be noted that electron beams during their transportation in the air (between the accelerator output unit and the plane of potential placement of irradiated samples) can generate secondary bremsstrahlung photons due to the bremsstrahlung process [7]. The thickness of the air layer to the potential plane of sample placement can vary depending on the geometric dimensions of the beams (increasing the distance to the samples is necessary to ensure the uniformity of the electron beam field [3]).

Reliable data on the content of secondary photons and their characteristics in electron accelerator beams are extremely important for the development of radiation technologies. This data is primarily necessary for developing innovative methods for minimizing the content of photons in electron beams [8] and for forming mixed electron-photon fields for radiation treatment of irradiated objects [9-11]. In addition, it is necessary for the development of experimental methods to determine the dosimetric characteristics of electron beams from the generated secondary radiation in cases where direct measurements of these quantities are impossible [2,12,13]. An example of such research is the use of secondary photons generated by an electron beam [14].

As a result of the analysis of the available experimental and theoretical studies of the influence of air on the change in the characteristics of electron beams and generated secondary photons, it was found that these changes will significantly depend on the parameters of the primary (initial) electron beam [2,15]. The characteristics of electron sources are determined by two main parameters: the size of the output beam and the average energy. They significantly affect the dosimetric characteristics of the beam during transportation in the air to the plane of the irradiation objects [16]. The characteristics of the generated secondary photons also depend on the initial parameters of the electron beam [15]. Any differences between the characteristics of electron beams and generated secondary photons falling into the plane of the irradiation samples on different types of accelerators are caused by the technical parameters of their output nodes, which affect the final shape of the resulting dose distributions [15].

Therefore, for the successful use of electron accelerators to ensure the process of irradiation of samples and the ability to predict results, reliable data is required for each type of accelerator on the characteristics of their beams (electrons and secondary photons) interacting with the irradiation objects.

The purpose of this (presented) work was to study the influence of the air layer between the electron output node of the M-30 microtron and the plane in the potential placement of samples for irradiation on the characteristics of the initial electron beams with an energy of 17.5 MeV and the generated secondary photons.

MATERIALS AND METHODS

The simulation was performed for an uncollimated electron beam with an initial energy of 17.5 MeV since the use of additional structural elements in the sample irradiation schemes (for example, collimators, aligning filters) leads to additional contamination of the electron beam with secondary (generated) particles - electrons and photons [19]. When performing the calculations, an equally probable distribution of the initial electron beam over the plane (ellipse shape with axes of 22 and 6 mm) was set [18, 20]. A photograph of the electron output unit of the M-30 microtron in the air is presented in Fig. 1.

During the simulations, electrons and the bremsstrahlung photons generated by them were recorded, falling into the plane of potential installation of the studied samples (1000×1000 mm) at 13 fixed distances (1; 50; 100; 500; 1000; 1500; 2000; 2500; 3000; 3500; 4000; 4500 and 5000 mm) between the

output node and the plane of potential installation of the sample for irradiation. When performing calculations, the initial number of electrons was equal to 10^7. The results of the simulations – the energy spectra of electrons, secondary photons, and their integral values were normalized to one initial electron.

Fig. 1. Electron output unit of the M-30 microtron

RESEARCH RESULTS

As a result of the conducted computer experiment, the influence of the air layer between the electron output node of the M-30 microtron and the plane of potential installation of samples for irradiation on the spectral and integral characteristics of the initial electron beams and the secondary photons generated by them was investigated.

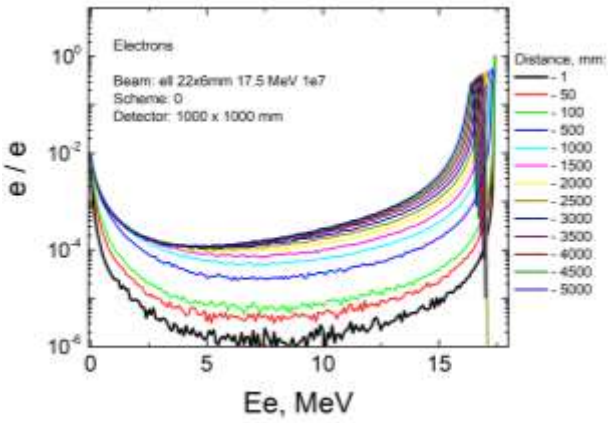

a

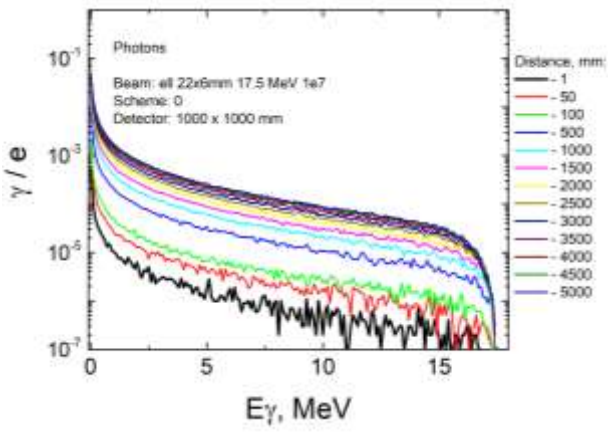

b

Fig. 2. Dependence of the energy spectra of electrons (a) and secondary photons (b) hitting the plane (1000×1000 mm) on the distances

Thus, the dependences of the energy spectra of electrons and generated secondary photons falling into the plane of the potential installation of samples from distances of 1…5000 mm, i.e., on different thicknesses of the air layers with which they interact, were established (Fig. 2).

The obtained energy spectra of electrons and secondary photons were used to calculate their integral values (Fig. 3, Table). Additionally, Table shows the dependence of the content values (in %) of secondary photons in the electron beam on the distance.

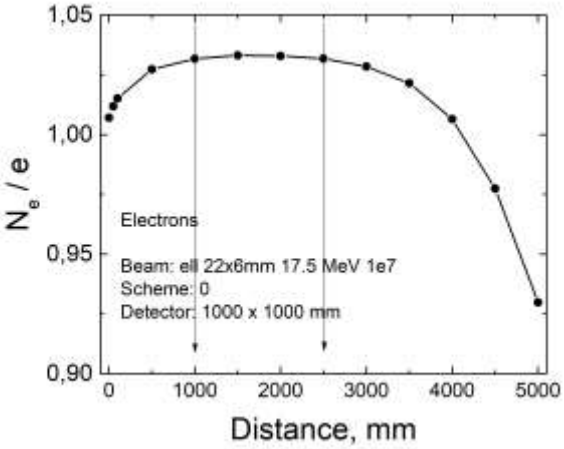

a

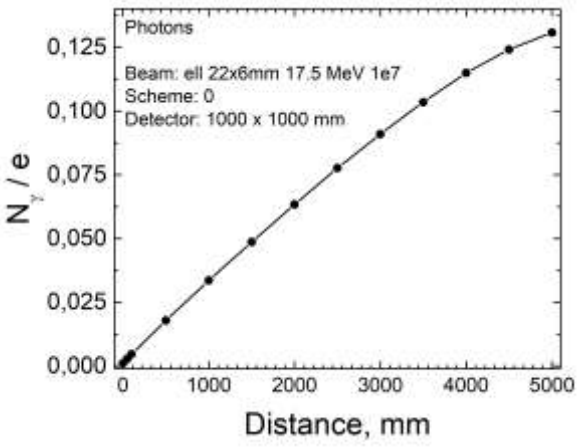

b

Fig. 3. Dependence of the integral values of electrons (a) and secondary photons (b) hitting the 1000×1000 plane on the distance

Analysis of the obtained spectral and integral characteristics of electrons and generated secondary photons indicates their significant dependence on distance (thickness of the air layer through which they are transported).

Due to the interaction of the primary electron beam with air layers (collision, ionization, scattering, and bremsstrahlung processes [21, 22]), significant changes occur in the characteristics of the primary (initial) electron beams and secondary photons generated in the air.

As the distance increases from 1 to 5000 mm, the maximum energy of electrons entering the plane decreases from 17.5 to ~ 16.4 MeV. Thus, for – 1 mm –

17.5 MeV, 1000 mm ~ 17.2 MeV, 2000 mm ~ 17.1 MeV, 3000 mm ~ 16.8 MeV, 4000 mm ~ 16.6 MeV, 5000 mm ~ 16.4 MeV.

Integral values of electrons and secondary photons falling into the plane at fixed distances

Distance, mm	Electrons total / e	Photons total / e	Photons % in beam
1	1.0071	0.0010	0.1012
50	1.0118	0.0028	0.2730
100	1.0151	0.0046	0.4501
500	1.0272	0.0179	1.7089
1000	1.0317	0.0336	3.1513
1500	1.0331	0.0487	4.4972
2000	1.0329	0.0633	5.7779
2500	1.0317	0.0776	6.9977
3000	1.0284	0.0910	8.1275
3500	1.0215	0.1035	9.2010
4000	1.0065	0.1150	10.2505
4500	0.9775	0.1242	11.2713
5000	0.9298	0.1308	12.3319

The integral value of electrons falling into the plane also significantly depends on the distance to it. Thus, these values increase in the range from 1 mm to ~ 1000 mm, and they practically do not change (almost the same) for the range from ~ 1000 to ~ 2500 mm and decrease from 2500 to 5000 mm.

Increasing the distance to the plane increases the probability of secondary photon generation due to the bremsstrahlung process of electrons in the air. The integral values of the generated secondary photons increase by ~ 128 times with increasing distance from 1 to 5000 mm – i.e., they are determined by the thickness of the air layer. The content of secondary photons in the electron beam increases from ~ 0.1 to ~ 12%.

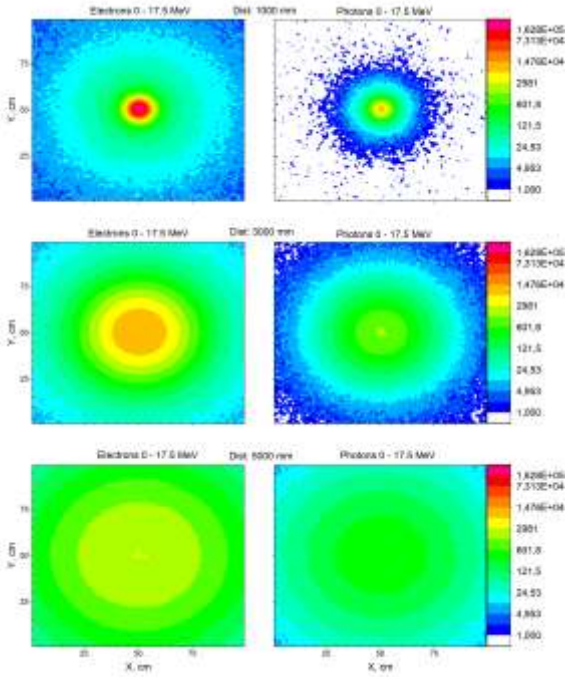

Fig. 4. Profiles of electrons and secondary photons incident on the plane at fixed distances – 1000, 3000, and 5000 mm

The simulation results allowed us to obtain profiles of electron beams and generated secondary photons in a section on planes of size 1000×1000 mm at fixed distances of 1000, 3000, and 5000 mm. A probability map of the distribution of electrons and secondary photons on the plane according to the inverse cumulative Gaussian distribution was created. The profiles of electrons and secondary photons falling into the plane of installation of the samples are presented in Fig. 4.

From the obtained simulation results, it was found that at a distance of 1000 mm from the output node, the highest concentration of electrons is in a plane with a radius of 40 mm, while for secondary photons, this radius is 20 mm with a concentration twice less than that of electrons. Further increase in distance leads to a gradual increase in the uniformity of the intensity of the electron and photon beam along the plane. This significantly reduces the number of particles hitting the irradiated target if it is on the beam axis.

The obtained results reflect the general patterns of the influence of air layers on the spectral, integral, and spatial distributions of primary electron beams and secondary photons and are close to the existing literature data [2, 15, 23, 24] obtained on different types of accelerators. Any differences between the corresponding specified characteristics are caused by the technical parameters of the accelerators (electron output nodes into the air), which significantly affect the kinetic parameters of electron beams and secondary photons in the plane of sample placement [2, 15].

CONCLUSIONS

As a result of the simulations conducted using the GEANT4 tool, the influence of air layers (between the electron output node of the M-30 microtron and the potential plane) on the characteristics of the primary electron beam with an energy of 17.5 MeV and secondary photons was established.

The results obtained will allow optimization of the process of sample irradiation and prediction of the results of experimental studies at the electron accelerator of the IEF of the NAS of Ukraine - microtron M-30.

This work was carried out within the framework of the topic "Excitation, ionization, luminescence of atomic and molecular systems under the action of photons and electrons," State Registration No. – 0124U000782.

REFERENCES

1. A.G. Chmielewski. Radiation technologies: The future is today // *Radiation Physics and Chemistry,* 2023, v. 213, p. 111233.
2. A. Ryczkowski, T. Piotrowski, M. Staszczak, et al. Optimization of the regularization parameter in the dual annealing method used for the reconstruction of energy spectrum of electron beam generated by the AQURE mobile accelerator // *Zeitschrift für Medizinische Physik.* 2024, v. 34, Is. 4, p. 510-520.

3. P. Apiwattanakul, S. Rimjae. Electron beam dynamic study and Monte Carlo simulation of accelerator-based irradiation system for natural rubber vulcanization // *Nuclear Inst. and Methods in Physics Research B*. 2020, v. 466, p. 69-75.
4. NIST ESTAR Database Program. https://physics.nist.gov/PhysRefData/Star/Text/ESTAR.html
5. Z. Yüksel, M.Ç. Tufan. Estimating the effect of electron beams interactions with the biological tissues //*Canadian Journal of Physics.* 2018, v. 96, No 12, p. 1338–1348.
6. M.K. Saadi, R. Machrafi. Development of a new code for stopping power and CSDA range calculation of incident charged particles, part A: Electron and positron // *Applied Radiation and Isotopes*. 2020, v. 161, p. 109145.
7. H.O. Tekina, T. Manici, E.E. Altunsoy, et al. An artificial neural network-based estimation of bremsstarahlung photon flux calculated by MCNPX // *Acta Physica Polonica A.* 2017, v. 132, p. 967-969.
8. G.X. Ding, Z.(J) Chen, K. Homann. A scattering-foil free electron beam to increase dose rate for total skin electron therapy (TSET) // *Medical Physics.* 2024, v. 51, p. 5563-5571.
9. N. Khaledi, D. Sardari, M. Mohammadi, et al. Dosimetric evaluation of a novel electron–photon mixed beam, produced by a medical linear accelerator // *Journal of Radiotherapy in Practice*. 2018, v. 17, p. 319-331.
10. V.A. Shevchenko, A.Eh. Tenishev, V.L. Uvarov, A.A. Zakharchenko. Operation of an industrial electron accelerator in a double-beam e,X-mode // *Problems of Atomic Science and Technology.* 2019, v. 124, N 6, p. 163-167.
11. V.L. Uvarov, A.A. Zakharchenko, L.V. Zarochintsev, et al. Analysis of a double-beam e,X-modeat an idustrial accelerator “EPOS” // *Problems of Atomic Science and Technology.* 2020, v. 127, №3, p. 154-157.
12. R.I. Pomatsalyuk, V.A. Shevchenko, D.V. Titov, et al. Formation and monitoring of secondary x-ray radiation under product processing with electron beam // *Problems of Atomic Science and Technology.* 2021. v. 136, № 6, p. 201-205.
13. C. Oancea, K. Sykorova, J. Jakubek, et al. Dosimetric and temporal beam characterization of individual pulses in FLASH radiotherapy using Timepix3 pixelated detector placed out-of-field // *Physica Medica*. 2025, v. 129, p. 104872.
14. H. Kim, D.H. Jeong, S.K. Kang, et al. Real-time monitoring of ultra-high dose rate electron beams using bremsstrahlung photons // *Nuclear Engineering and Technology.* 2023 v. 55, p. 3417-3422.
15. A. Ryczkowski, B. Pawałowski, M. Kruszyna-Mochalska, et al. Commissioning, dosimetric characterisation and machine performance assessment of the AQURE mobile accelerator for intraoperative radiotherapy // *Polish Journal of Medical Physics and Engineering.* 2024, v. 30, p. 177-181.
16. L. Grevillot, T. Frisson, D. Maneval, et al. Simulation of a 6 MV Elekta precise linac photon beam using GATE/GEANT4 // *Phys. Med. Biol.* 2011, v. 56, p. 903-918.
17. GEANT4 11.1 (9 December 2022). https://geant4.web.cern.ch/support/download
18. E.V. Oleinikov, I.V. Pylypchynets, O.O. Parlag, V.V. Pyskach. Photon and photoneutron outputs simulation from a tantalum converter at the M-30 microtron // *Problems of Atomic Science and Technology.* 2024. v. 153, № 5, p. 148-153.
19. A. Toutaoui, A.N. Aichouche, K. Adjidir, A.C. Chami. In-air fluence profiles and water depth dose for uncollimated electron beams // *Journal of Medical Physics*. 2008, v. 33, p 141-146.
20. M.I. Romanyuk, J.J. Gaynish, O.M. Turhovsky, et al. Methods of formation and control of radiation fields of M-30 microtron // *Journal of Physical Studies.* 2022, v. 26, p. 1201.
21. S. Kahane. Backscattering of MeV Electrons. An Analysis of Tabata’s experiment with Geant4 // *European Journal of Applied Physics*. 2022, v. 4, p. 48-56.
22. B. Koohi, R. Khabaz. Study of the backscattering of electron beams with energies typical of radiotherapy // *Physica Scripta.* 2022, v. 97, p. 125301.
23. G.X. Ding, Z.(J) Chen, K. Homann. A scattering-foil free electron beam to increase dose rate for total skin electron therapy (TSET) // *Medical Physics.* 2024, v. 51, p. 5563-5571.
24. G.X. Ding, S. Kucuker-Dogan, I.J. Das. Brems-strahlung dose in the electron beam at extended distances in total skin electron therapy // *Medical Physics,* 2022, v. 49, issue 2, p. 1297-1302.